An Evaluation of The Neocognitron

David R. Lovell, *Member, IEEE,* Thomas Downs, *Member, IEEE,* and Ah Chung Tsoi, *Senior Member, IEEE*

***Abstract*—We describe a sequence of experiments investigating the strengths and limitations of Fukushima's neocognitron as a handwritten digit classifier. Using the results of these experiments as a foundation, we propose and evaluate improvements to Fukushima's original network in an effort to obtain higher recognition performance. The neocognitron's performance is shown to be strongly dependent on the choice of selectivity parameters and we present two methods to adjust these variables. Performance of the network under the more effective of the two new selectivity adjustment techniques suggests that the network fails to exploit the features that distinguish different classes of input data. To avoid this shortcoming, the network's final layer cells were replaced by a nonlinear classifier (a multilayer perceptron) to create a hybrid architecture. Tests of Fukushima's original system and the novel systems proposed in this paper suggest that it may be difficult for the neocognitron to achieve the performance of existing digit classifiers due to its reliance upon the supervisor's choice of selectivity parameters and training data. These findings pertain to Fukushima's *implementation* of the system and should not be seen as diminishing the practical significance of the concept of hierarchical feature extraction embodied in the neocognitron.**

***Index Terms*— Handwritten character recognition, neocognitron, selectivity**

I. Introduction

THE *NEOCOGNITRON* [1]–[7] is a massively parallel, hierarchical neural network, designed, primarily, for two-dimensional (2-D) pattern recognition. Proposed by Fukushima in 1979 [1], it was inspired by Hubel and Wiesel's serial model of biological vision [8] and, for the last decade, it has been acclaimed as a shift and distortion tolerant character recognition system.

Some of the neocognitron's biological plausibility was sacrificed in 1983 when Fukushima moved away from the original paradigm of self-organization and introduced a supervised training scheme in an effort to improve the network's handwritten character recognition performance [2]. However, to the best of our knowledge, there have been no concrete performance statistics published to indicate whether the desired improvement was achieved. Unlike Hubel and Wiesel's serial model of vision, which has undergone rigorous scrutiny to test its validity, the capabilities of the neocognitron have not been critically reviewed to any significant extent.

Manuscript received Sepbemter 11, 1995; revised August 12, 1996, January 1, 1997, and May 4, 1997.

D. R. Lovell is with the Department of Engineering, University of Cambridge, Cambridge CB2 1PZ, U.K.

T. Downs is with the Department of Electrical and Computer Engineering, University of Queensland, Queensland 4072, Australia.

A. C. Tsoi is with the Faculty of Informatics, University of Wollongong, Northfields Avenue, Wollongong, NSW 2522, Australia.

Publisher Item Identifier S 1045-9227(97)06050-5.

The neocognitron was proposed well before multilayer perceptrons and backpropagation became popular. Why has so little independent empirical research been published on this system? One reason may be the relative complexity of the network (as mentioned in [9, p. 199], [10, p. 187]) and, in light of this, we present a review of the neocognitron's operation (Section II) followed by a concise definition of the system (Section III). (A less mathematical review is given in [9].)

In Section IV, we examine how the neocognitron calculates the similarity between an input pattern and the pattern classes it has been trained to identify. Section IV highlights the importance of S-cell *selectivity* in obtaining good performance from the network.

Hildebrandt's method for adjusting selectivities is briefly reviewed in Section V before two new techniques are presented and evaluated using real-world digit data. The most effective of these methods is used as a basis for further improvements to the neocognitron—described in Section VI—in which the distinguishing features of different classes of digits are exploited to achieve more accurate classification. Effectively, in Section VI, we attempt to fine tune the neocognitron to maximize recognition performance.

The paper concludes with a review of the empirical results obtained and the implications they have for the neocognitron, and its variants, as practical digit recognition systems.

II. Overview of the Neocognitron

The neocognitron classifies input through a succession of functionally equivalent stages. Each stage extracts "appropriate" features from the output of the preceding stage and forms a compressed representation of those extracted features. This representation preserves the spatial location of the extracted features and becomes the input to the next stage.

Classification is achieved by steadily extracting and compressing feature representations until the input is transformed into a vector whose elements are measures of the similarity between the input pattern and the input classes that the neocognitron has been trained to recognize. In a *winner-take-all* fashion, the final layer unit with the highest output determines the class assigned to an input pattern.

Feature extraction is performed by arrays of *S-cells* (called *S-planes*) trained to respond to certain features *deemed by the supervisor* to characterize input patterns. Each S-cell receives input from a rectangular region of cells in each *C-cell* plane (*C-plane*) of the preceding stage. The set of weights between each S-cell and its input regions is the same for every S-cell within a given plane. This *weight sharing* ensures features are detected wherever they lie in the input cell plane.

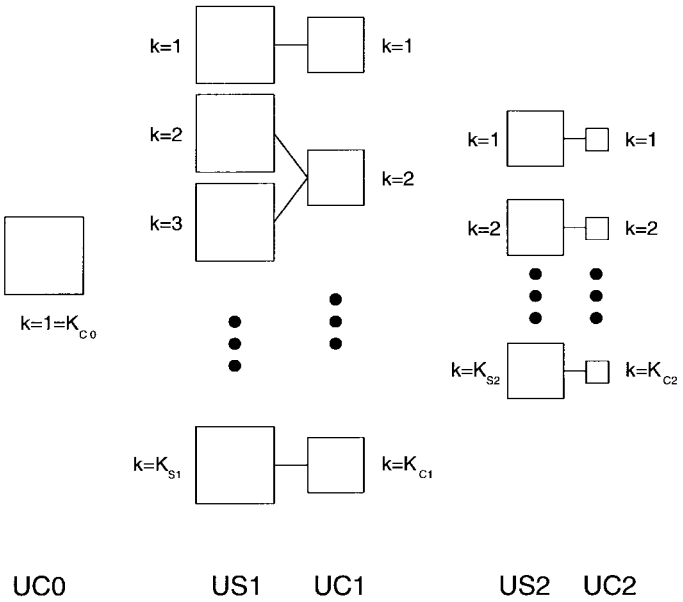

Fig. 1. Cell-planes are identified by a serial number k. When necessary to refer to two cell-planes in different layers, Fukushima uses κ to denote the second serial number. Layers of S-planes are labeled US1, US2, etc., while layers of C-planes are labeled UC0, UC1 and so on.

C-plane activity is a compressed approximation of the activity in the preceding S-planes. This compression of representation also provides a degree of translational invariance to the neocognitron [11].

III. Formal Definition of the Neocognitron

Despite the neocognitron's complexity, its formal description can still be organized into a logical progression of concepts. We address three major issues:

1) the *organization* of the cells in the neocognitron;
2) the *interconnections* between them;
3) the *functional description* of those cells.

We have adopted Fukushima's system of terminology (used in almost all neocognitron literature) but, for the sake of both completeness and clarity, new notation to describe training patterns is introduced in Section III-C (completeness) and abbreviated vector notation is defined in Section IV (clarity).

Since its inception, certain aspects of the neocognitron have been altered by Fukushima. We shall adhere to Fukushima's most recent *complete* description of the neocognitron [4] in the following discussion.

A. The "Morphology" of the Neocognitron

There are *three* types of processing element in the neocognitron: S-cells, C-cells, and V-cells. Any individual S or C-cell is identified by four pieces of information:

- the *type* of cell (S or C);
- the *layer*, ℓ, that the cell belongs to;
- the *cell-plane*, k, that it is part of
- the *location*, $\boldsymbol{n}$, of the cell within that cell-plane.

The outputs of S and C-cells are given the general notation $u_{S\ell}(\boldsymbol{n}, k)$ and $u_{C\ell}(\boldsymbol{n}, k)$.

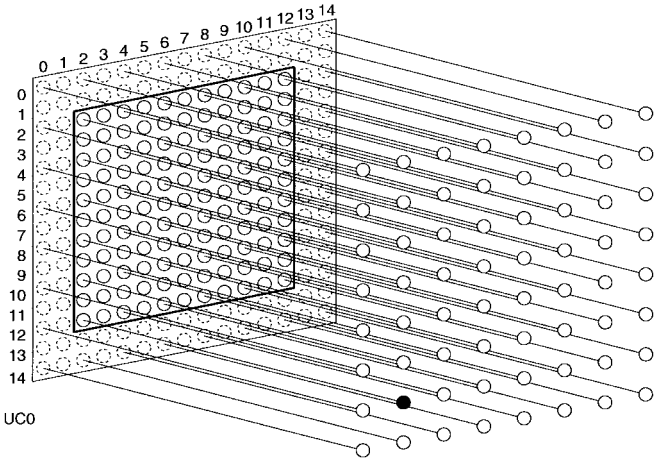

Fig. 2. A cell's position within its plane is given by the coordinates of its projection onto the input cell plane. This projection is the center of the cell's receptive field and may lie outside the physical input cell-plane, UC0. Here the UC0 plane is 11×11 cells in size and the location of the black cell is at $n = (2, 12)$.

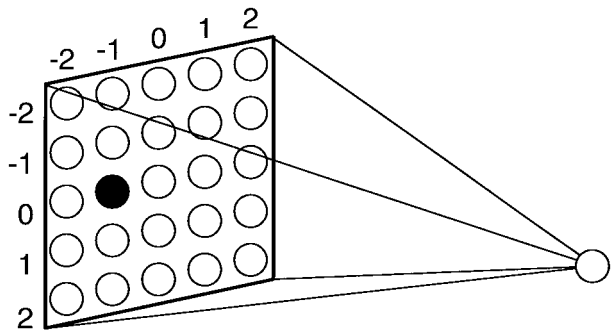

Fig. 3. The weight sharing mechanism used in the neocognitron makes it convenient to specify a particular connection in terms of ν, the position of a source cell within a destination cell's input region. In this 5×5 cell input region the black cell is at $\nu = (-1, 0)$.

V-cells provide information to S-cells about the amount of activity present within each S-cell's input regions. Only one V-cell plane (*V-plane*) per layer is necessary to store the values of weighted root-mean-square input region activity (see Fig. 4), hence a particular V-cell is specified by

- the *type* of cell (i.e., V);
- the *layer*, ℓ, that the cell belongs to;
- the *location*, $\boldsymbol{n}$, of the cell within the V-plane.

The outputs of V-cells are given the general notation $u_{V\ell}(\boldsymbol{n})$.

The possible values of parameters ℓ, k and $\boldsymbol{n}$ are determined by the architecture of a specific network. In layer ℓ, S-planes are numbered one to $K_{S\ell}$; C-planes range from one to $K_{C\ell}$ (see Fig. 1). A cell's location within an S, C or V-plane is specified by a 2-D position vector, $\boldsymbol{n}$. This vector describes the position of a cell's receptive field center in relation to the input cell plane, UC0, as depicted in Fig. 2.

B. The Synaptic Organization of the Neocognitron

The neocognitron is structured like a large sandwich of alternating S and C-plane layers. Only adjacent layers of cell-planes are directly connected and an S-cell is connected with

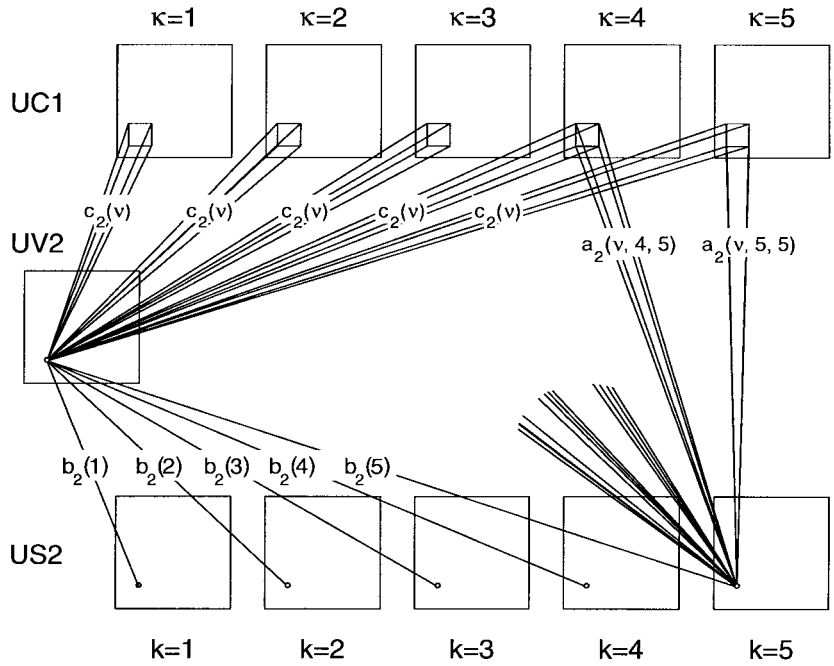

Fig. 4. V-cells have fixed weight links from input regions in all immediately preceding C-planes. Each V-cell's output is approximately equal to the magnitude of activity within its input regions. In layer ℓ, every cell in S-plane k receives inputs from a V-cell that has the same input regions. The strength of this input is weighted by the inhibitory coefficient $b_\ell(k)$.

cells in all immediately preceding C-planes. Individual links from C-cells to an S-cell[1] are identified by four pieces of information

- the *layer*, ℓ, of the S-plane that they connect to;
- the *serial number*, k, of that S-plane;
- the *serial number*, κ, of the C-plane from which the link originates;
- the *location*, $\boldsymbol{\nu}$, within the connection region, A_ℓ, of the C-cell from which the link originates.

Weights from C to S-cells are given the general notation $a_\ell(\boldsymbol{\nu}, \kappa, k)$. Since all cells in S-plane k share the same weights, the connection $a_\ell(\boldsymbol{\nu}, \kappa, k)$ does *not* contain the argument $\boldsymbol{n}$ to define a specific S-cell as the destination of that link. The location of a link's source cell is identified by the position vector $\boldsymbol{\nu}$ (see Fig. 3). S-cell weights have nonnegative values, as do all other weights and parameters in the neocognitron.

S-cells also receive input from subsidiary V-cells (Fig. 4). The degree that V-cells affect cells in a given S-plane, k, is determined by the positive value of the *inhibitory coefficient* $b_\ell(k)$.

Fig. 4 shows that V-cells are linked with preceding C-planes in the same way that S-cells are. Unlike C-plane to S-cell weights though, connections between C-planes and any V-cell are fixed and specified as a function of a C-cell's position, $\boldsymbol{\nu}$, within the connection region A_ℓ. Each of the sets of weights (or *masks*) between a V-cell in layer ℓ and the previous C-planes is denoted $c_\ell(\boldsymbol{\nu})$.

Connections from S-cells to a C-cell are also fixed and expressed as a function of S-cell position within a C-cell input region, D_ℓ. A set of S-cell to C-cell weights is given the notation $d_\ell(\boldsymbol{\nu})$. Since a particular C-plane may receive input from one or more S-planes, S to C-plane connectivity is described by the factor $j(\kappa, k)$. If S-plane κ and C-plane k are connected, then $j(\kappa, k) > 0$, otherwise[2], $j(\kappa, k) = 0$.

The notation defined so far does not provide a way to express the spatial relationships and interconnectivity between cells. Rather than formalize this issue with more definitions, Fukushima presents this information diagrammatically, as shown in Fig. 5. For simplicity, this diagram presents connection information as though there were but a single S and C-plane in each layer of the network—links between additional cell-planes obey the same scheme of interconnection. Fig. 5 shows how the ratios of S and C-cells in layers two, three and four cause activity to converge to a single cell. Overlapping connections ensure this compression is achieved without undersampling. Note that the finite width of cell planes can cause cells at the edge of a plane to receive only partial connection to the previous layer.

C. The "Cytology" of the Neocognitron

Now the naming conventions used by Fukushima have been presented, we can define the equations governing S, C, and V-cell function and the rules specifying the evolution of weights in the neocognitron. This section is deliberately terse; explanation of the following equations is relegated to Section IV so that *definition* and *interpretation* of cell function can remain distinct.

[1]The prepositions *to* and *from* specify the direction of information flow along a connection between cells. The output of a *source* cell flows *to* a *destination* cell; a destination cell receives input *from* a source cell.

[2]Fukushima implies that the actual value of $j(\kappa, k)$ for connected cell-planes is one [4].

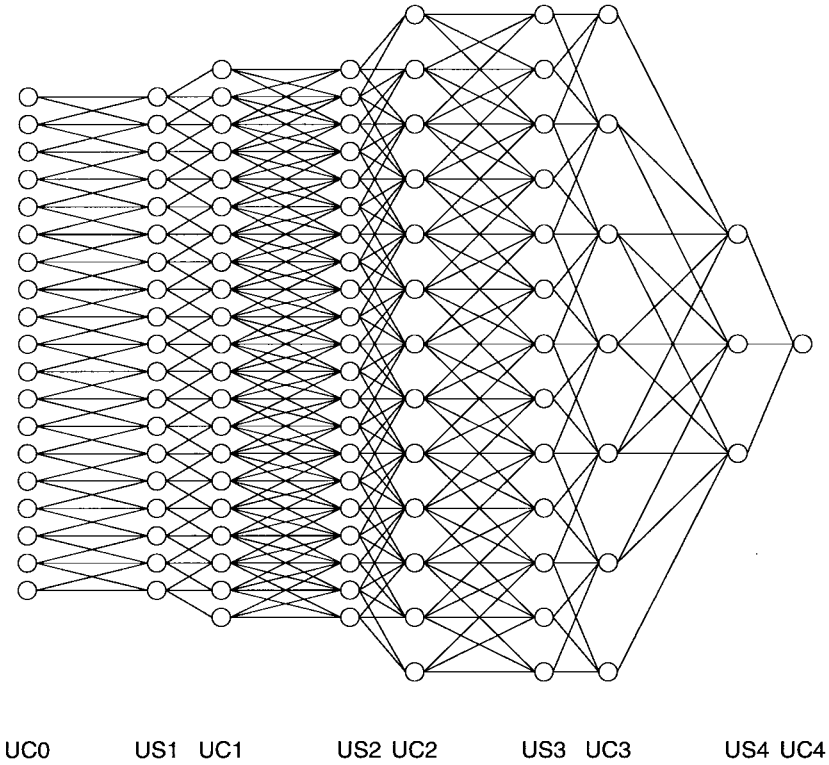

Fig. 5. This two dimensional "slice" through the neocognitron shows the interconnections between one S and C-plane from each layer of the network. It shows, for instance, how each of the cells in a 13× 13 layer 2 C-plane receives input from different 7 × 7 cell regions in the preceding layer 2 S-plane. This figure is based on the network described in [3].

The output of an S-cell in the kth S-plane of the ℓth layer of the neocognitron is given by

$$u_{S\ell}(\boldsymbol{n},k) \stackrel{\text{def}}{=} r_\ell \left[\frac{1+\sum_{\kappa=1}^{K_{C\ell-1}}\sum_{\boldsymbol{\nu}\in A_\ell} a_\ell(\boldsymbol{\nu},\kappa,k)\cdot u_{C\ell-1}(\boldsymbol{n}+\boldsymbol{\nu},\kappa)}{1+\frac{r_\ell}{r_\ell+1}\cdot b_\ell(k)\cdot u_{V\ell}(\boldsymbol{n})}-1\right]. \quad (1)$$

The function $\varphi(\cdot)$ is a *threshold-linear* transfer function, defined by

$$\varphi(x) \stackrel{\text{def}}{=} \begin{cases} 0 & \text{if } x<0 \\ x & \text{if } 0\le x. \end{cases} \quad (2)$$

The *selectivity parameter*, r_ℓ, determines how closely the cell's input must correspond to the inputs it has been trained with in order to elicit a response.

The double summation in the numerator of (1) is a *weighted sum* of the outputs of C-cells in the preceding layer. C-cell output is expressed as

$$u_{C\ell}(\boldsymbol{n},k) \stackrel{\text{def}}{=} \psi\left[\sum_{\kappa=1}^{K_{S\ell}} j(\kappa,k)\cdot\sum_{\boldsymbol{\nu}\in D_\ell} d_\ell(\boldsymbol{\nu})\cdot u_{S\ell}(\boldsymbol{n}+\boldsymbol{\nu},\kappa)\right] \quad (3)$$

where

$$\psi(x) \stackrel{\text{def}}{=} \frac{\varphi(x)}{1+\varphi(x)}. \quad (4)$$

The transfer function, $\psi(\cdot)$, limits C-cell output to the range [0, 1).

V-cells have an inhibitory effect and *normalize* an S-cell's response with respect to its input region activity. A V-cell's output is equal to the weighted root-mean-square value of the C-cell activity within its input regions

$$u_{V\ell}(\boldsymbol{n}) \stackrel{\text{def}}{=} \sqrt{\sum_{\kappa=1}^{K_{C\ell-1}}\sum_{\boldsymbol{\nu}\in A_\ell} c_\ell(\boldsymbol{\nu})\cdot u^2_{C\ell-1}(\boldsymbol{n}+\boldsymbol{\nu},\kappa)}. \quad (5)$$

There are four different kinds of weights used in the neocognitron: $a_\ell(\boldsymbol{\nu},\kappa,k), b_\ell(k), c_\ell(\boldsymbol{\nu})$ and $d_\ell(\boldsymbol{\nu})$. The first two of these are determined during training, the last two are specified as

$$c_\ell(\boldsymbol{\nu}) = \gamma_\ell^{|\boldsymbol{\nu}|} \quad (6)$$

$$d_\ell(\boldsymbol{\nu}) = \overline{\delta}_\ell\cdot\delta_\ell^{|\boldsymbol{\nu}|} \quad (7)$$

where $0<\gamma_\ell,\delta_\ell\le 1$ and $0<\overline{\delta}_\ell$.

Algorithm 1 uses pseudocode to describe the training of the neocognitron; this allows us to present modifications to Fukushima's learning algorithm as straightforwardly as possible. To present Fukushima's *supervised* training algorithm[3] in this way, it is necessary to define further notation for the training exemplars.

Supervised training of the neocognitron requires that each S-plane be exposed to one or more training patterns. We define

[3]Supervised training produces better recognition performance than self-organization [2] and since we are interested in maximizing the neocognitron's performance we shall only discuss this so-called *training-with-a-teacher* method of learning. The reader is referred to [12] for information about unsupervised learning in the neocognitron.

the set of training patterns for S-plane k in layer ℓ as

$$t_{k\ell} \stackrel{\text{def}}{=} \{t_{k\ell 1}, \cdots, t_{k\ell m}, \cdots, t_{k\ell_{|t_{k\ell}|}}\} \tag{8}$$

where $|t_{k\ell}|$ is the number of elements in $t_{k\ell}$. The *seed-cell* $\boldsymbol{n}_{k\ell m}$ is associated with the mth training pattern. Both training patterns and their corresponding seed-cell locations are specified by the supervisor.

Assuming that all connections described by $a_\ell(\boldsymbol{\nu}, \kappa, k)$ and $b_\ell(k)$ are initially equal to zero, the process of training a neocognitron with layers 1 to L can be written as shown in Algorithm 1 at the bottom of the page.

The procedure $activate(\ell)$ represents the propagation of activity from the S-cell inputs to the C-cell outputs of layer ℓ, according to the transformations defined by (1)–(5). The parameter q_ℓ is a positive number known as the *learning rate* of layer ℓ. Note that this algorithm is completely deterministic.

This concludes the formal specification of the neocognitron but there is still much more to tell. Several people (including Fukushima) have analyzed how the neocognitron extracts features [13]–[15]. The following section gives an interpretation of (1)–(7) and establishes concepts which will be useful to us later.

IV. The Calculation of Similarity

The neocognitron is based on the notion of similarity. On a small scale, individual S-cells calculate the similarity between the patterns of activity in their input regions and the features to which they have been trained to respond. On a large scale, the outputs of the neocognitron represent the similarities between the input pattern and each of the different input classes that the network has been trained to recognize. Only the similarity calculated by S-cells has a direct mathematical representation as in (1). This representation has a geometrical interpretation, with weights and inputs represented in Euclidean space. Before rendering this view of S-cell behavior, we must define some additional vector notation.

If the connection region of an ℓth layer S-cell is defined as the set of all input cell position vectors in a preceding C-plane, i.e.,

$$A_\ell \stackrel{\text{def}}{=} \{\boldsymbol{\nu}_1, \boldsymbol{\nu}_2, \cdots, \boldsymbol{\nu}_{|A_\ell|}\} \tag{9}$$

then the weight, mask, and input vector of any cell in the kth S-plane of layer ℓ can be written as

$$\boldsymbol{a}_\ell \stackrel{\text{def}}{=} \begin{bmatrix} a_\ell(\boldsymbol{\nu}_1, 1, k) \\ \vdots \\ a_\ell(\boldsymbol{\nu}_{|A_\ell|}, 1, k) \\ a_\ell(\boldsymbol{\nu}_1, 2, k) \\ \vdots \\ a_\ell(\boldsymbol{\nu}_{|A_\ell|}, 2, k) \\ \vdots \\ a_\ell(\boldsymbol{\nu}_{|A_\ell|}, K_{C\ell-1}, k) \end{bmatrix}$$

$$\boldsymbol{c}_\ell \stackrel{\text{def}}{=} \begin{bmatrix} c_\ell(1) \\ \vdots \\ c_\ell(|A_\ell|) \\ c_\ell(1) \\ \vdots \\ c_\ell(|A_\ell|) \\ \vdots \\ c_\ell(|A_\ell|) \end{bmatrix}$$

Algorithm 1: Fukushima's Supervised Training Algorithm

procedure $train\_neocognitron()\{$
  for $\ell = 1$ **to** L $\{$ # For each layer of the neocognitron
    $train\_layer(\ell)$; # learn S-cell weights.
  $\}$
$\}$
procedure $train\_layer(\ell)$ $\{$ # Update S-plane weights
  for $k = 1$ **to** $K_{S\ell}$ $\{$ # for each S-plane in layer ℓ *and*
    for $m = 1$ **to** $|t_{k\ell}|$ $\{$ # for each training pattern of the kth S-plane.
      $UC0 = t_{k\ell m}$; # Load the mth pattern into the input plane,
      for $layer = 0$ **to** $\ell - 1$ $\{$ # propagate activity from input to layer $\ell - 1$,
        $activate(layer)$;
      $\}$
      $train\_S\_cell(\boldsymbol{n}_{k\ell m}, k, \ell)$; # then update the weights of the seed cell.
    $\}$
  $\}$
$\}$
procedure $train\_S\_cell(\boldsymbol{n}_{k\ell m}, k, \ell)$ $\{$ # Update the $a_\ell(\boldsymbol{\nu}, \kappa, k)$ and $b_\ell(k)$ weights
  for $\kappa = 1$ **to** $K_{C\ell-1}$ $\{$ # for each C-plane in the preceding layer
    for all $\boldsymbol{\nu} \in A_\ell$ $\{$ # and for all input region cell positions.
      $a_\ell(\boldsymbol{\nu}, \kappa, k) = a_\ell(\boldsymbol{\nu}, \kappa, k) + q_\ell \cdot c_\ell(\boldsymbol{\nu}) \cdot u_{C\ell-1}(\boldsymbol{n}_{k\ell m} + \boldsymbol{\nu}, \kappa)$;
    $\}$
  $\}$
  $b_\ell(k) = b_\ell(k) + q_\ell \cdot u_{V\ell}(\boldsymbol{n}_{k\ell m})$;
$\}$

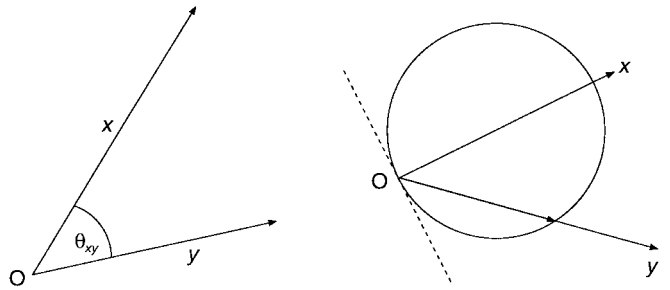

(a) (b)

Fig. 6. (a) A two-dimensional example of vectors x, y and the angle between them, θ_{xy}. (b) The locus of $\cos\theta_{xy} \cdot \hat{y}$ as y takes all possible directions in the plane.

and

$$\boldsymbol{u}_{C\ell-1} \stackrel{\text{def}}{=} \begin{bmatrix} u_{C\ell-1}(\boldsymbol{n}+\boldsymbol{\nu}_1,1) \\ \vdots \\ u_{C\ell-1}(\boldsymbol{n}+\boldsymbol{\nu}_{|A_\ell|},1) \\ u_{C\ell-1}(\boldsymbol{n}+\boldsymbol{\nu}_1,2) \\ \vdots \\ u_{C\ell-1}(\boldsymbol{n}+\boldsymbol{\nu}_{|A_\ell|},2) \\ \vdots \\ u_{C\ell-1}(\boldsymbol{n}+\boldsymbol{\nu}_{|A_\ell|},K_{C\ell-1}) \end{bmatrix}$$

respectively. The vector of seed-cell inputs corresponding to the mth training pattern of the kth S-plane in layer ℓ is denoted by

$$\boldsymbol{u}^m_{C\ell-1} \stackrel{\text{def}}{=} \begin{bmatrix} u_{C\ell-1}(\boldsymbol{n}_{klm}+\boldsymbol{\nu}_1,1) \\ u_{C\ell-1}(\boldsymbol{n}_{klm}+\boldsymbol{\nu}_2,1) \\ \vdots \\ u_{C\ell-1}(\boldsymbol{n}_{klm}+\boldsymbol{\nu}_{|A_\ell|},1) \\ u_{C\ell-1}(\boldsymbol{n}_{klm}+\boldsymbol{\nu}_1,2) \\ u_{C\ell-1}(\boldsymbol{n}_{klm}+\boldsymbol{\nu}_2,2) \\ \vdots \\ u_{C\ell-1}(\boldsymbol{n}_{klm}+\boldsymbol{\nu}_{|A_\ell|},2) \\ \vdots \\ u_{C\ell-1}(\boldsymbol{n}_{klm}+\boldsymbol{\nu}_{|A_\ell|},K_{C\ell-1}) \end{bmatrix}.$$

The inputs and weights of an S-cell are vectors in *pattern space* and a convenient measure of their similarity is the *cosine* of the angle between them. The degree of similarity between these two vectors is defined as

$$s(\boldsymbol{a}_\ell, \boldsymbol{u}_{C\ell-1}) \stackrel{\text{def}}{=} \frac{\boldsymbol{a}_\ell^T \boldsymbol{u}_{C\ell-1}}{|\boldsymbol{a}_\ell||\boldsymbol{u}_{C\ell-1}|} \tag{10}$$

that is, the cosine of $\theta_{\boldsymbol{a}_\ell \boldsymbol{u}_{C\ell-1}}$ [see Fig. 6(a)]. Fig. 6(b) shows a 2-dimensional example of the *direction cosine* surface described when the similarity measure of vectors $\boldsymbol{x}$ and $\boldsymbol{y}$ is projected in the direction of $\boldsymbol{y}$.

Since there may be no activity within a cell's input regions (i.e., every element of $\boldsymbol{u}_{C\ell-1}$ could be zero), (10) cannot be used directly as a similarity measure. The S-cell function described in (1) is based upon a variation of (11)

$$s'(\boldsymbol{a}_\ell, \boldsymbol{u}_{C\ell-1}) \stackrel{\text{def}}{=} \frac{1+\boldsymbol{a}_\ell^T \boldsymbol{u}_{C\ell-1}}{1+|\boldsymbol{a}_\ell||\boldsymbol{u}_{C\ell-1}|}. \tag{11}$$

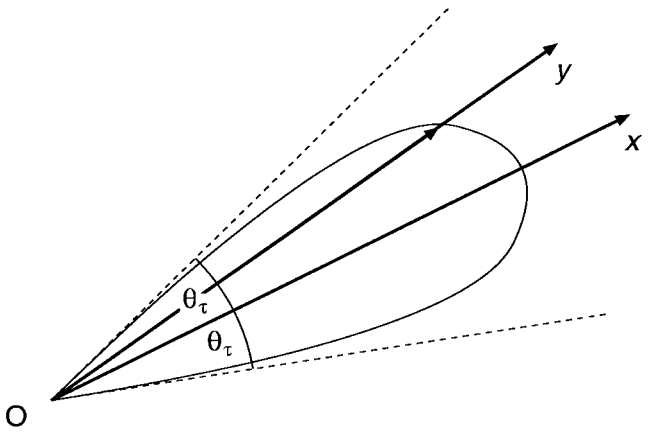

Fig. 7. The locus of $s''(x,y)\cdot\hat{y}$ for all directions of y. Since $\theta_\tau = \cos^{-1}\tau$, the higher the threshold, the narrower the locus about x becomes. Thus, high values of τ restrict the range of input vectors for which $s''(x,y)$ is greater than zero (i.e., the *acceptance region*, $\mathcal{A}$). In two dimensions, $\mathcal{A}$ is a triangular region (between the dotted lines above), in three dimensions it is conical, and in higher dimensions the shape of the acceptance region is described as a *hypercone*.

This modified similarity measure avoids the problem of zero length input vectors and is approximately equal to the similarity measure of (10) when $|\boldsymbol{a}_\ell||\boldsymbol{u}_{C\ell-1}| \gg 1$ (a condition which can be assured by using a large learning rate, e.g., $q_\ell \approx 10^5$ as suggested in [4]). The relation between (1) and (11) is not immediately apparent; subsequent equations should clarify the situation.

The purpose of an S-cell is to respond to an input *sufficiently* similar to the patterns it has been trained with. Fukushima has incorporated (11) into the mathematical description of the S-cell so the degree of input and weight vector similarity necessary for nonzero S-cell response can be adjusted. By introducing a *threshold* parameter, $\tau \in [-1,1]$, and a threshold-linear transfer function as in (2), a further measure of similarity can be defined by

$$s''(\boldsymbol{a}_\ell, \boldsymbol{u}_{C\ell-1}) \stackrel{\text{def}}{=} \varphi\left[\frac{s'(\boldsymbol{a}_\ell, \boldsymbol{u}_{C\ell-1})-\tau}{1-\tau}\right]. \tag{12}$$

If $s'(\boldsymbol{a}_\ell, \boldsymbol{u}_{C\ell-1}) \le \tau$, the nonnegative function $\varphi(\cdot)$ ensures $s''(\boldsymbol{a}_\ell, \boldsymbol{u}_{C\ell-1}) = 0$. If, however, the weight and input vectors are similar enough that $s'(\boldsymbol{a}_\ell, \boldsymbol{u}_{C\ell-1}) > \tau$ then $0 < s''(\boldsymbol{a}_\ell, \boldsymbol{u}_{C\ell-1}) \le 1$. Since $s'(\boldsymbol{a}_\ell, \boldsymbol{u}_{C\ell-1}) \approx \cos\theta_{\boldsymbol{a}_\ell \boldsymbol{u}_{C\ell-1}}$ (for $|\boldsymbol{a}_\ell|\boldsymbol{u}_{C\ell-1}| \gg 1$), the parameter τ defines a *threshold angle*, $\theta_\tau = \cos^{-1}\tau$. Fig. 7 is a geometrical interpretation of (12) and shows how τ can control the range of input vectors that make $s''(\cdot)$ positive. The volume of pattern space in which $s''(\cdot) > 0$ is referred to as the *acceptance region*, $\mathcal{A}$.

Equation (12) and parameter τ do not appear in other literature about the neocognitron. Instead of τ, Fukushima's S-cell description uses a *selectivity parameter*, r, to regulate the acceptance region. The threshold parameter is related to this quantity by $\tau = r/(r+1)$, where $r \ge -0.5$, hence

$$\begin{aligned} s''(\boldsymbol{a}_\ell, \boldsymbol{u}_{C\ell-1}) &= \varphi\left[\frac{s'(\boldsymbol{a}_\ell, \boldsymbol{u}_{C\ell-1}) - \dfrac{r}{r+1}}{1-\dfrac{r}{r+1}}\right] \\ &= \varphi[(r+1)s'(\boldsymbol{a}_\ell, \boldsymbol{u}_{C\ell-1}) - r] \end{aligned} \tag{13}$$

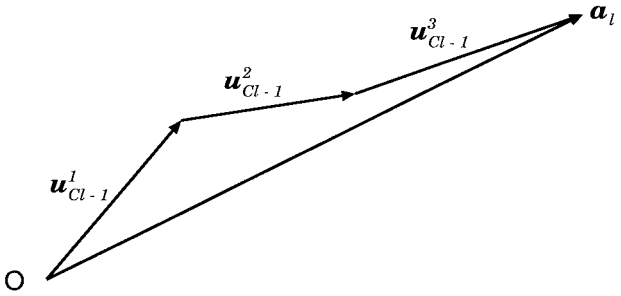

Fig. 8. Once training is complete, an S-cell's weight vector a_ℓ is proportional to the vector sum of the inputs presented during training $u^1_{C\ell-1} + u^2_{C\ell-1} + \cdots$.

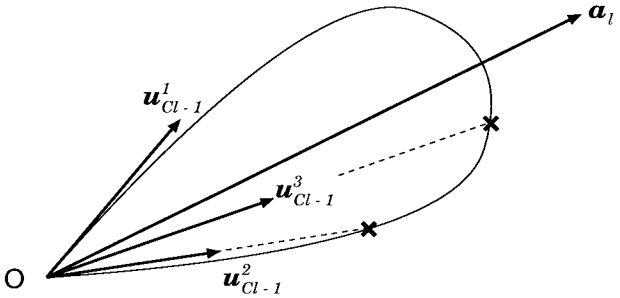

Fig. 10. For a given training pattern, the output of the S-cell is equal to the length of the line from the origin to the locus of S-cell output (the teardrop shaped lobe) in the direction of the appropriate input vector.

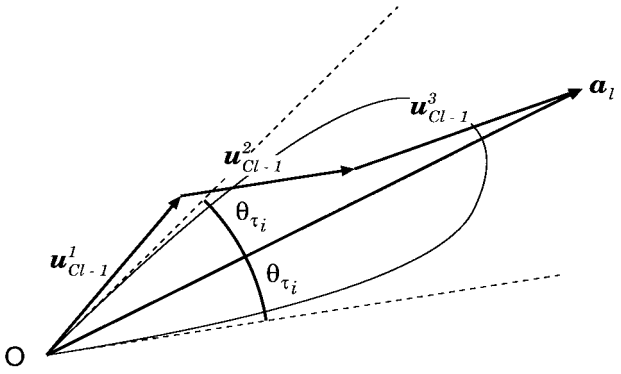

Fig. 9. If selectivity is chosen independently of training vectors, there is a risk of setting r_ℓ so high that one or more training vectors falls outside the acceptance region, as is the case for exemplar $u^1_{C\ell-1}$.

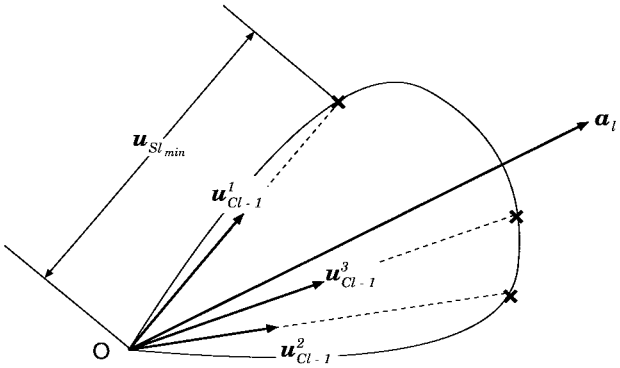

Fig. 11. SOFT adjusts the S-cell's selectivity to ensure the smallest output, in response to a training vector, is equal to $u_{S\ell_{\min}}$. Note the increased response of the S-cell to the second and third training patterns.

and, using some algebraic manipulation and the fact that $\varphi(r \cdot z) = r \cdot \varphi(z)$ for positive values of r, it can be shown that this equation is approximately equal to (1).

What (13) and Fig. 7 show is that S-cell output (and hence network classification performance) depends strongly on selectivity. A high value of selectivity will cause an S-cell's acceptance region to be quite acute—the cell will only respond to inputs highly similar to the patterns with which it was trained. Low selectivity produces a broad acceptance region and an S-cell that will respond to a wide range of inputs—possibly inputs quite unlike those it was trained to recognize. In the next section we consider how to adjust selectivity to maximize recognition.

V. Adjusting Selectivity

Hildebrandt [15] was the first to propose a comprehensive[4] scheme for adjusting S-cell selectivities. However, for reasons not initially apparent, Hildebrandt's optimal closed-form training (OCFT) algorithm failed to produce a network that performed well.

Without going into great detail,[5] the central idea of OCFT is to adjust S-cell selectivity so the acceptance regions of cells in different S-planes (within a given layer) are as large as possible without overlapping. Hildebrandt reasoned that this would allow S-cells to tolerate the largest amount of distortion in input without compromising their ability to discriminate.

[4] Selectivity adjustment was discussed briefly in [12].

[5] OCFT and its mode of failure are discussed fully in [16] and [17].

In practice [16], it was found that OCFT adjusted selectivities so that some S-cells would fail to recognize even the exemplars they were trained with, severely degrading overall performance. This *training feature rejection* occurred because OCFT determines selectivities on the basis of the *average* of S-plane training features. OCFT does not guarantee that selectivity will be adjusted so *individual* training vectors lie within the appropriate acceptance regions (as depicted in Figs. 8 and 9).

A. Suboptimal Feature-Based Training

One solution to the problem of training feature rejection is to adjust S-cell selectivity to *guarantee* a minimum S-cell response to *all* training patterns. This is the basis of the suboptimal feature-based training (SOFT) algorithm described here.

The strategy of SOFT is to scale an S-cell's response to a training feature by adjusting the cell's selectivity from its initial value. This adjustment is carried out using the training pattern which elicits the weakest response from the S-cell. Using the general notation of Sections III and IV, the output of the seed cell in the kth S-plane of layer ℓ, in response to the mth training pattern, is $u_{S\ell}(\boldsymbol{n}_{k\ell m}, k)$. The initial selectivity of that cell is $r_{k\ell}$. We define the weakest response to a training pattern for this S-plane as

$$\min_{u_{S\ell}(k)} \stackrel{\text{def}}{=} \min_m u_{S\ell}(\boldsymbol{n}_{k\ell m}, k). \tag{14}$$

SOFT adjusts the selectivity of the S-cell from $r_{k\ell}$ to $r'_{k\ell}$ so that the weakest S-cell response to a training pattern becomes

$u_{S\ell_{\min}}$. The parameter $u_{S\ell_{\min}}$ is referred to as the *guaranteed minimum S-cell response* and satisfies $0 < u_{S\ell_{\min}} < 1$.

To explain how SOFT adjusts selectivity, we need to define S-cell *activation* as

$$x_{S\ell}(\boldsymbol{n}, k) \stackrel{\text{def}}{=} (r_{k\ell} + 1)s'(\boldsymbol{a}_\ell, \boldsymbol{u}_{C\ell-1}) - r_{k\ell} \tag{15}$$

which is essentially the argument of $\varphi[\cdot]$ in (13). In a similar fashion to (14), the minimum S-cell activation in response to a training vector is defined as

$$\min_{x_{S\ell}(k)} \stackrel{\text{def}}{=} \min_m \; x_{S\ell}(\boldsymbol{n}_{k\ell m}, k). \tag{16}$$

From (11) we know $s'(\boldsymbol{a}_\ell, \boldsymbol{u}_{C\ell-1})$ depends only on the angle formed between the vector of inputs to an S-cell, $\boldsymbol{u}_{C\ell-1}$, and that cell's weight vector, $\boldsymbol{a}_\ell$. Using (15), we can calculate what the modified similarity measure of an S-cell must be, given that the activation and selectivity of the cell are $\min_{x_{S\ell}(k)}$ and $r_{k\ell}$, respectively:

$$s'(\boldsymbol{a}_\ell, \boldsymbol{u}_{C\ell-1}) = \frac{r_{k\ell} + \min_{x_{S\ell}(k)}}{r_{k\ell} + 1}. \tag{17}$$

The goal of SOFT is to adjust $r_{k\ell}$ to $r'_{k\ell}$ so that $\min_{x_{S\ell}(k)} = u_{S\ell_{\min}}$. This means that

$$u_{S\ell_{\min}} = (r'_{k\ell} + 1)s'(\boldsymbol{a}_\ell, \boldsymbol{u}_{C\ell-1}) - r'_{k\ell}. \tag{18}$$

Rearranging this to isolate the required selectivity value gives

$$r'_{k\ell} = \frac{s'(\boldsymbol{a}_\ell, \boldsymbol{u}_{C\ell-1}) - u_{S\ell_{\min}}}{1 - s'(\boldsymbol{a}_\ell, \boldsymbol{u}_{C\ell-1})} \tag{19}$$

and substituting in (17) gives an explicit expression for the value of $r'_{k\ell}$ in terms of the current selectivity and cell activation, and the desired output:

$$r'_{k\ell} = \frac{\left(\dfrac{r_{k\ell} + \min_{x_{S\ell}(k)}}{r_{k\ell} + 1}\right) - u_{S\ell_{\min}}}{1 - \left(\dfrac{r_{k\ell} + \min_{x_{S\ell}(k)}}{r_{k\ell} + 1}\right)}. \tag{20}$$

Now we can incorporate (20) into a precise specification of the SOFT algorithm (see Algorithm 2 at the bottom of the page).

As with Fukushima's supervised training algorithm, this training scheme commences with all connections $a_\ell(\boldsymbol{\nu}, \kappa, k)$ and $b_\ell(k)$ set to zero, as shown in Algorithm 2.

B. Implementation Issues with SOFT

While SOFT alleviates the problem of training feature rejection, its implementation requires that three additional issues be addressed.

1) Instead of eliminating (or even reducing) the number of parameters that need to be chosen, SOFT *replaces* the set of selectivity parameters with a set of guaranteed minimum S-cell response parameters. We have no guidelines as to how to choose suitable values of $u_{S\ell_{\min}}$ (see Fig. 12).
2) We cannot apply SOFT to S-cells that have only one training pattern (Fig. 13). After training is complete, an S-cell with only one training pattern will have the

---

Algorithm 2: (The Suboptimal Feature-based Training Algorithm

procedure $train\_neocognitron()$ {
  for $\ell = 1$ **to** L {; # For each layer of the neocognitron
    $train\_layer(\ell)$; # learn S-cell weights
    $tune\_layer(\ell)$; # then adjust S-cell selectivities.
  }
}
procedure $tune\_layer(\ell)$ { # Tune the selectivities
  for $k = 1$ **to** $K_{S\ell}$ { # for each S-plane in layer ℓ.
    $r_{k\ell} = 1$; # Initialize selectivity of the kth S-plane,
    $\min_{x_{S\ell}(k)} = 1$; # initialize minimum S-cell response, and
    for $m = 1$ **to** $|t_{k\ell}|$ { # for each training pattern of
      # the kth S-plane
      $UC0 = t_{k\ell m}$; # load the mth pattern into the input plane
      for $layer = 0$ **to** ℓ { # and propagate activity from input$\cdots$
        $activate(layer)$; # to layer ℓ.
      }
      # If seed-cell's activation < current minimum then
      # update the current minimum S-cell response.
      if $x_{S\ell}(\boldsymbol{n}_{k\ell m}, k) < \min_{x_{S\ell}(k)}$ **then**
      $\min_{x_{S\ell}(k)} = x_{S\ell}(\boldsymbol{n}_{k\ell m}, \kappa)$;
    }
    # Adjust $r_{k\ell}$ so that the minimum S-cell response
    # to any training pattern will be $u_{S\ell_{\min}}$.
    $r_{k\ell} = \left(\dfrac{r_{k\ell} + \min_{x_{S\ell}(k)}}{r_{k\ell} + 1} - u_{S\ell_{\min}}\right) \Big/ \left(1 - \dfrac{r_{k\ell} + \min_{x_{S\ell}(k)}}{r_{k\ell} + 1}\right)$;
  }
}

TABLE I
IN THIS COMPARATIVE TABLE "KF-1988" REFERS TO THE NETWORK DESCRIBED IN [3], "DL-1992" IS THE NETWORK DESCRIBED IN [17]. RECOGNITION RELIABILITY IS DEFINED AS THE PROPORTION OF DIGITS CORRECTLY CLASSIFIED OUT OF ALL DIGITS NOT REJECTED. IN EXPERIMENT 9, THE MLP SECTION OF THE NETWORK WAS TRAINED WITH 4840 CEDAR DIGITS, WITH 4400 CEDAR DIGITS USED AS A VALIDATION SET TO DETERMINE WHEN TO STOP TRAINING

Expt	Network	Training Alg.	Test Data	Size	Correct	Wrong	Reject	Reliability
1	KF-1988	Algorithm 1	Lovell's	400	52.50%	26.25%	21.25%	66.67%
2	KF-1988	**OCFT**	Lovell's	400	3.25%	10.00%	86.75%	24.53%
3	KF-1988	**SOFT**	Lovell's	400	74.00%	26.00%	0.00%	74.00%
4	KF-1988	**SOFT**	CEDAR	400	47.25%	52.00%	0.25%	47.61%
5	KF-1988	**SOFT**	CEDAR (thinned)	400	51.50%	48.50%	0.00%	51.50%
6	DL-1992	**SOFT**	CEDAR	400	55.75%	26.75%	17.50%	67.58%
7	DL-1992	**SOFT**	CEDAR (thinned)	400	58.75%	26.00%	15.25%	69.32%
8	DL-1992	**SHOP**	CEDAR (thinned)	400	75.75%	23.75%	0.50%	76.13%
9	**NCMLP**	**SHOP** + BP	CEDAR	2711	84.73%	3.14%	12.13%	96.43%

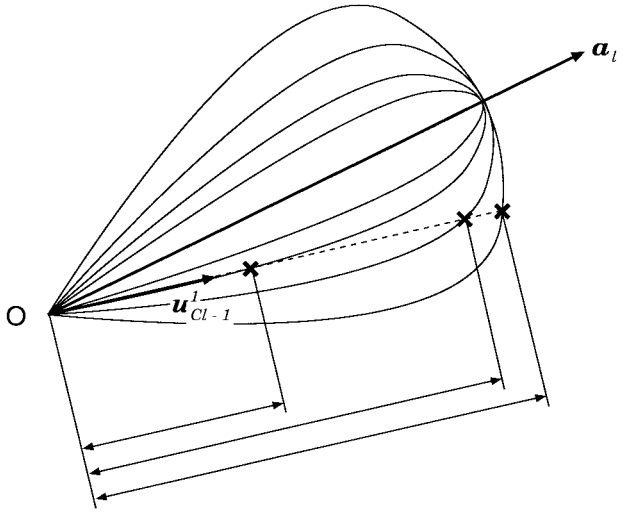

Fig. 12. By varying $r_{k\ell}$, we can produce a family of S-cell output loci, giving a range of feasible $u_{S\ell_{\min}}$ values. This figure shows how three different choices of $r_{k\ell}$ give three different nonzero S-cell outputs for the input vector $u^1_{C\ell-1}$. It is unclear which choice is best.

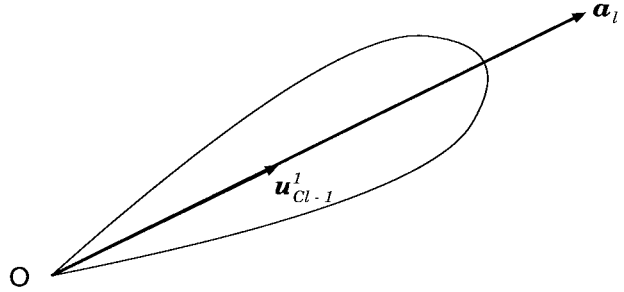

Fig. 13. If an S-cell has a single training vector, the cell's output in response to that vector will be one, regardless of the value of selectivity.

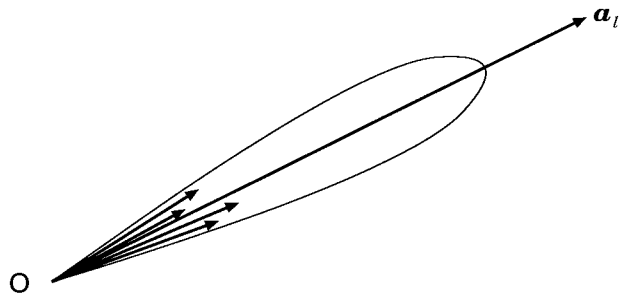

Fig. 14. Highly similar training vectors cause SOFT to produce a highly selective S-cell.

weights $\boldsymbol{a}_\ell = q_\ell\ \boldsymbol{u}^1_{C\ell-1}$, and when we compute this cell's activation in response to its training vector we have $x_{S\ell}(\boldsymbol{n}_{k\ell 1}, k) = 1$. Equation (20) shows that this activation means $r'_{k\ell} \to \infty$ (for $0 \le u_{S\ell_{\min}} < 1$). If it were possible to implement such a value of $r'_{k\ell}$, the S-cell would respond only when the inputs to the cell were identical to the cell's weight vector, effectively removing any capacity for that S-cell to generalize.

3) The experimenter's choice of training features indirectly determines S-cell selectivity. A set of highly similar training vectors will produce an S-cell with a very narrow acceptance region. Certainly, all training vectors will elicit a nonzero response from that S-cell, but, unless the actual distribution of *typical* features is tightly clumped within the acceptance region, the cell will be far too selective (Fig. 14).

On the other hand, a training vector substantially dissimilar to other training vectors will cause an S-cell's acceptance region to balloon out to encompass it (Fig. 15). An S-cell with such a low selectivity will be responsive to almost any feature and, therefore, probably not be of much use within the neocognitron. To use Hildebrandt's terms, finding the appropriate balance between generalization and discrimination is still a problem.

In the next section we determine whether these problems are a major handicap in applying SOFT to the neocognitron.

C. Experiments with SOFT

As experiments with OCFT demonstrated [16], the effect of any changes to a complex system like the neocognitron must

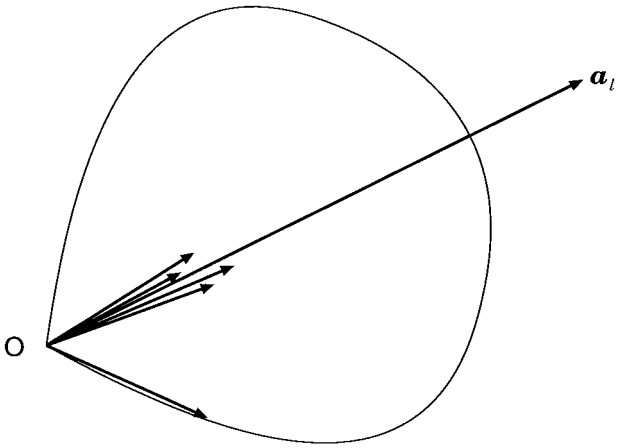

Fig. 15. One unusual training feature will radically alter the acceptance region produced by SOFT.

be assessed empirically. Table I shows the performance of the neocognitron for a variety of architectures, training algorithms and test data.

Initially, we did not have access to a database of test digits so a set of 400 digits was "constructed" by the first author.[6] Under the assumption that test set performance is binomially distributed, this size of test set provides estimates within $\pm 5\%$ of the network's true recognition rate with 95% confidence.

Our first experiment (results of which were independently verified [18]) evaluated the performance of the neocognitron described by Fukushima[7] in 1988 [3]. (We refer to this version of the neocognitron as "KF-1988".) We then assessed this KF-1988's performance after OCFT and it became clear that Hildebrandt's scheme had some shortcomings (see rows 1 and 2 of Table I).

The next step was to apply SOFT to KF-1988—this presented two difficulties. First, a number of S-planes (including all first layer S-planes) within Fukushima's network had single training patterns; we decided not to adjust the selectivities of these planes. Given that one of the final layer S-planes had a single training pattern, we also decided to set $r_4 = 1.0$ to ensure that all S-planes in the final layer had equal sized acceptance regions.

Second, we had to choose guaranteed minimum S-cell response parameters for layers 2 and 3 of the network. In the absence of any firm guidelines, we set $u_{S2_{\min}} = 0.5$ and $u_{S3_{\min}} = 0.75$.

As shown in row 3 of Table I, SOFT boosted the classification rate of Fukushima's network by over 20%. However, when this system was evaluated on real world data from the CEDAR database[8] [19]. it was clear that the "constructed" testing data was considerably easier to classify than actual handwritten digits (compare rows 3, 4, and 5 of Table I).

[6] Lovell's test digits are public domain and are currently available via e-mail (contact `drl@eng.cam.ac.uk`).

[7] We gratefully acknowledge Prof. Fukushima's kind assistance in providing us with his training data.

[8] Test data was drawn from the `TEST/BINDIGIS/BS` directory of the CD-ROM. Full details of the exact digits used and the preprocessing that was applied to them are given in [17, Appendix B]

Handwritten character recognition systems often *thin* data before attempting classification. Row 5 of Table I shows thinning[9] gives a slight improvement in performance. To further enhance recognition, a new set of training patterns (based on features present in CEDAR database training digits) was created and a new network structure was implemented. (Full details of this new architecture—referred to as "DL-1992"—and also its training data are given in [17, Appendixes B and C].) The performance obtained is shown in rows 6 and 7 of Table I. The degree of improvement makes it seem unlikely that SOFT could produce a neocognitron able to correctly classify around 90% of real-world digits, with near 100% reliability—levels of performance obtained by other digit recognition systems [21], [22].

SOFT represents a significant improvement upon OCFT and salvages some of the ideas put forward by Hildebrandt. However, it is the authors' conviction that the geometric assumptions upon which OCFT and SOFT are based, should be put aside.

D. Selectivity Hunting to Optimize Performance

If OCFT and SOFT are not the best selectivity adjustment techniques, what issues should be considered in designing an effective method? The experiments described above, as well as results of some additional tests, led us to conclude that a suitable algorithm has the following characteristics.

1) It needs to incorporate extensive amounts of real-world data into the adjustment process. Even though the neocognitron makes use of hand-crafted exemplars to determine S-cell weights, actual handwritten digits can still be used in the selectivity adjustment procedure.
2) It must utilize a meaningful performance measure during training, i.e., one directly related to the network's ability to generalize, not just its capacity to associate the correct output with each training pattern.
3) It should not be based on unnecessarily restrictive assumptions about the distribution of patterns or features in input space; both OCFT and SOFT have demonstrated the dangers of making assertions in this regard.
4) It must not introduce new parameters that have to be carefully chosen to obtain satisfactory behavior from the network.

Taking these points into consideration, we propose a simple method of selectivity adjustment called SHOP—selectivity hunting to optimize performance. The concept behind this new algorithm is to take a number of identically structured neocognitrons, with different selectivity parameters, train them (using the same set of exemplars), then see which one is best at classifying a validation set of handwritten digits; the ideal selectivities are taken to be those of the network with the highest classification performance on the validation set.

Obviously, such a naïve method for determining selectivities must be subject to certain constraints and assumptions for it to be feasible. Instead of attempting to individually adjust the selectivity of each S-plane, SHOP maximizes the classification performance of the network with the constraint that all S-

[9] Data was thinned using the Safe Point Thinning Algorithm [20].

planes within a given layer have the same selectivity value. Also, because S-cell selectivity is a continuous variable, SHOP relies upon *sampling* the range of possible selectivities to obtain a finite number of performance estimates for a specific neocognitron.

SHOP is described in Algorithm 3, where R_ℓ is the set of all ℓth layer selectivities to be considered when testing the performance of the neocognitron.

In the pseudocode (shown in Algorithm 3 at the bottom of the page) the procedure known as $train\_neocognitron()$ refers to Fukushima's original training algorithm (Algorithm 1).

The purpose of the $test\_neocognitron()$ procedure is to evaluate the performance of the network using a validation set of real-world data. It is up to the experimenter to decide exactly how the network's performance is to be measured. Correct classification rate and reliability are examples of statistics that could both be used to measure the network's performance as shown in Algorithm 3.

When the algorithm terminates, R_{best} contains the selectivities that elicited the highest performance from the network. These selectivities can then be used in practical implementations of the system.

E. Implementation Issues with SHOP

Although SHOP has the potential to make good use of real-world data and employs a more realistic measure of network performance than any of the algorithms discussed previously, the exhaustive search approach to finding a good set of selectivities has a number of drawbacks.

1) Execution time cannot be ignored in our assessment of SHOP's feasibility. If t_T is the time taken to train the neocognitron, t_P is the time taken to propagate activity through the network and N_V is the number of examples in the validation set, then the time taken to execute SHOP is

$$t_{\text{shop}} = |R_1| \times |R_2| \times \cdots \times |R_L| \times (t_T + N_V\, t_P).$$

Fukushima [4] cites values of $t_T = 780s, t_P = 3.3s$ for a simulation of the neocognitron, written in FORTRAN and running on a SUN Sparcstation. If we specified ten possible selectivity values for each layer of a four-layer network and used a validation set with 400 patterns, SHOP would take about eight months to come up with a good set of selectivities on Professor Fukushima's computer. In a commercial/industrial situation, a SHOP trained neocognitron would have to be implemented with dedicated hardware (e.g., [23]).

2) The success of SHOP relies upon the stability of the neocognitron's performance with respect to changes in selectivity. If small changes in the selectivity of any layer cause the performance of the neocognitron to fluctuate wildly, then sampling the net's performance for a variety of selectivities will be of little use to us.

F. Experiments with SHOP

As indicated in the previous section, execution time was a major concern in our experiments with SHOP. The duration of each experiment was reduced by two orders of magnitude by restricting the first- and fourth-layer selectivity values tested. Since the relation between the input pattern and the outputs of the first-layer S-planes was readily observable, a suitable r_1 value could be determined by trial and error. Hence, the set of first-layer selectivities to be tested contained only one value: $R_1 = \{1.7\}$.

With respect to final layer selectivity it is important to remember that, while r_4 determines the *value* of the outputs of the network, it has no effect on which of the outputs is the largest. Since input patterns are classified on a winner-take-all basis, r_4 tends not to affect the classification performance of the network (providing it is not so high as to make US4 cells reject a large proportion of input patterns). The arbitrary restriction of $R_4 = \{1.0\}$ did not appear to cause any problems in the tests on SHOP. As well as saving time, restriction of first- and fourth-layer selectivities allowed the classification

Algorithm 3: (The Selectivity Hunting to Optimize Performance Algorithm)

```
procedure SHOP() {
  for all r_1 ∈ R_1 {                    # Using every possible combination
   ⋮                                     # of selectivities,
    for all r_L ∈ R_L {                  # in all layers of the neocognitron,
      train_neocognitron();              # train the network···
      test_neocognitron();               # and then test it.
                                         # If the current network has
      if performance > best_so_far {     # the best performance (so far),
          best_so_far = performance;     # update the best performance value
          R_best = (r_1, r_2, ···, r_L); # and store the L-tuple of selectivities
      }                                  # used by the present network.
    }
   ⋮
  }
}
```

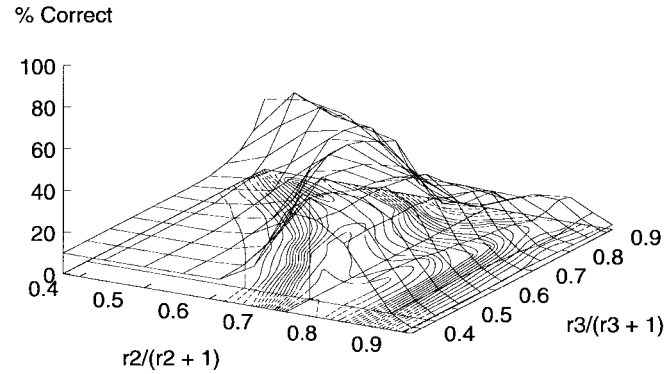

Fig. 16. The performance surface obtained with the KF-1988 network using a validation set of 400 unthinned CEDAR digits. Peak correct classification was 49.00% (54.60% reliability) for $r_2 = 2.563, r_3 = 0.7805$.

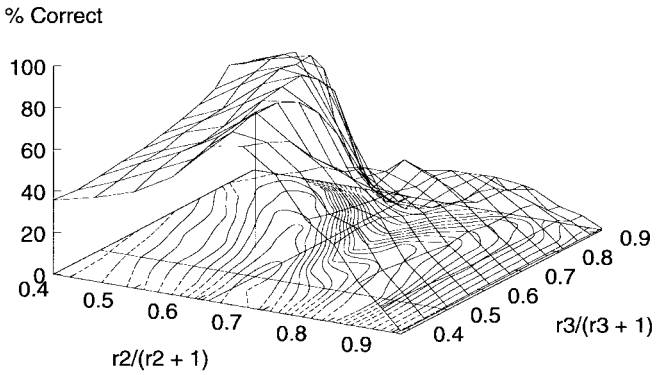

Fig. 18. The performance surface obtained with the DL-1992 network using a validation set of 400 unthinned CEDAR digits. A peak correct classification was 79.00% (79.42% reliability) for $r_2 = 1.602, r_3 = 1.000$.

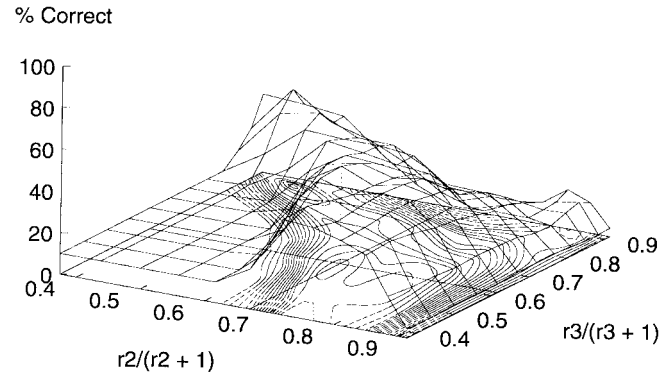

Fig. 17. The performance surface obtained with the KF-1988 1988 network using a validation set of 400 thinned CEDAR digits. Peak correct classification was 46.75% (49.34% reliability) for $r_2 = 2.022, r_3 = 1.602$.

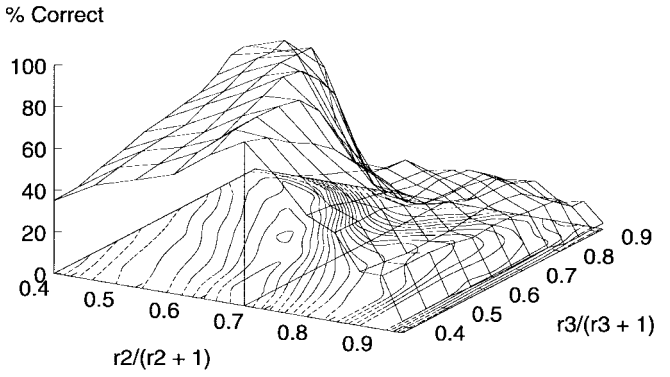

Fig. 19. The performance surface obtained with the DL-1992 network using a validation set of 400 thinned CEDAR digits. A peak correct classification was 78.75% (79.15% reliability) for $r_2 = 2.022, r_3 = 0.5990$.

performance of the network to be readily visualized as a *performance surface*—a function[10] of r_2 and r_3.

Figs. 16 and 17 show that peak recognition performances obtained using SHOP on Fukushima's 1988 network are fairly poor. We reasoned that this may have been due to the stylized digit fragments used to train this system so, to test this hypothesis, we applied SHOP to the DL-1992 network (which used more "realistic" digit fragments during training). Figs. 18 and 19 show this gave around 30% improvement in peak performance. Furthermore, the network's peak classification rate on the validation set of *unthinned* digits was slightly *in excess* of that achieved with the validation set of *thinned* digits—a finding contrary to Fukushima's comments that implied the the first layer of the neocognitron would have to be redesigned to cope with unthinned input patterns [4, Section V].

Performance surfaces are only useful if they can be used to *predict* good selectivity values. To see if this was the case, we compared the performance surface of Fig. 19 to that given by a test set of 400 thinned CEDAR digits. Not only was the correlation between these two surfaces high ($\rho = 0.9961$), the maxima of both surfaces was achieved with the same (r_2, r_3) combination: $r_2 = 2.022, r_3 = 0.5990$. SHOP appears to provide an accurate prediction of good selectivity values. The peak performance obtained with the test digits is shown in row 8 of Table I.

Since SHOP allows us to systematically evaluate the neocognitron's behavior, it can be used to investigate the effect of parameters other than selectivity. We know how to choose good values of selectivity (r_ℓ) and that the learning rate (q_ℓ) should be high, but we do not know how to choose the *mask parameters*, γ_ℓ, δ_ℓ and $\overline{\delta}_\ell$ [(6) and (7)] or even (as Hildebrandt suggested [15, Section III-B]) whether such parameters are necessary. To explore this issue, we set all mask parameters of the DL-1988 network to 1.0—effectively removing their influence on the network—and used SHOP with 400 thinned CEDAR digits to evaluate the network's performance surface. The surface obtained differed from the one shown in Fig. 19 but the *peak classification performance* was not significantly different (a peak correct classification rate of 78.00%, with 78.20% reliability, occurred for $r_2 = 1.000, r_3 = 1.269$). Mask parameters *do not* seem to have a significant effect on the peak performance attainable.

VI. Further Improvements to the Neocognitron

We have investigated all parameters that affect cell function in the neocognitron. We know that by using a high learning rate ($q_\ell \approx 10^5$), appropriate mask parameter values ($\gamma_\ell, \delta_\ell \approx$

[10] It is convenient to plot performance across regular increments of $r_\ell/(r_\ell + 1)$since this corresponds to a uniform sample of acceptance regions (see Section IV).

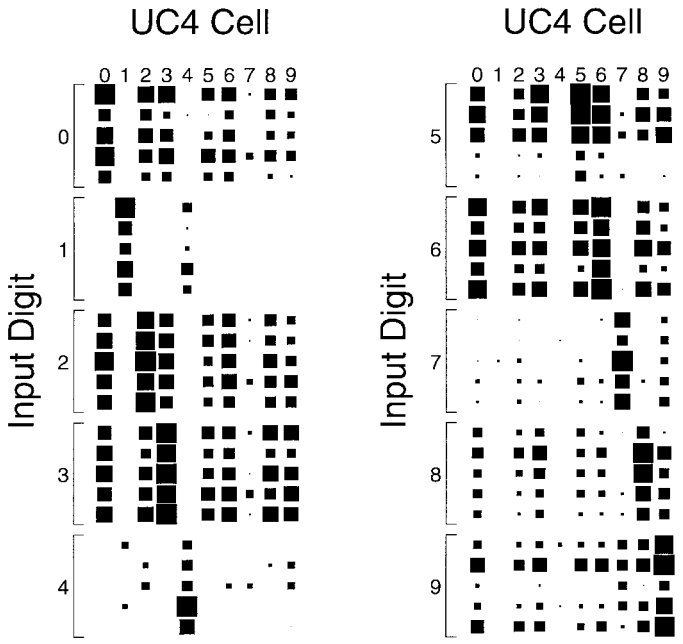

Fig. 20. Each row in the two large columns represents the outputs of the ten final layer C-cells in the DL-1992 network after training with SHOP using unthinned CEDAR digits (see Fig. 18). The class of input digit is indicated at the left of each column; UC4 cell numbers are shown at the top. The 50 digits that evoked these outputs were correctly classified. However, in many cases the margin between the largest and second largest output is small, making the classification vulnerable to error.

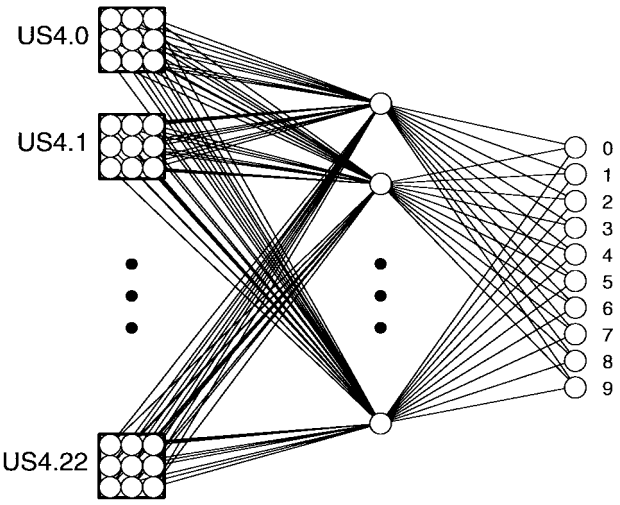

Fig. 21. The end portion of the **NCMLP** architecture. Final layer C-cells in a neocognitron are replaced by a two layer, fully connected MLP. The MLP receives input from the US4 cell planes and propagates activity through a layer of hidden units to the ten output units that indicate the **NCMLP**'s classification of the input image.

$0.71.0$; $\overline{\delta}_\ell \approx 1.04.0$) and selectivities determined by SHOP, a correct classification rate of around 76%, with 76% reliability, is feasible. If further improvement is to be achieved it seems we must alter the neocognitron to attain it.

Researchers often decompose the problem of handwritten character recognition into two stages. *Feature extraction* obtains some numerical (or logical) measure of the characteristics of the input image, then the image undergoes *classification* and is labeled (or rejected) on the basis of the features extracted. Our attention has been focussed mainly on the neocognitron's feature extracting abilities and we have tended to ignore the 1% of cells in the network (i.e., those in the final layer) that tell us what class has been assigned to an input pattern. For reasons explained in the previous section, SHOP does not alter the selectivities of these cells; examination of the network's outputs during operation gives an indication of the problems that occur as a result.

Fig. 20 shows typical levels of output activity for 50 correctly classified input digits. Clearly, the neocognitron is not discriminating *effectively* between different classes of input. The outputs, as with all other cells in the network, simply indicate the degree to which certain features are present in the input image. Should some of the features detected by one cell also be detected by others, a number of cells can show high levels of activity at the same time. Consequently, the neocognitron is apt to confuse certain digits (such as 2's and 3's) because of the number of features they have in common.

We need final layer cells to exploit the idiosyncratic aspects of each kind of digit to obtain more robust classification. The multilayer perceptron (MLP) has been popular as a *distribution free* classifier [24]. Perhaps coupling the neocognitron and MLP would create a system that could perform distortion tolerant feature extraction *and* robust classification? We refer to this hybrid system as the NCMLP (neocognitron plus MLP).

Put simply, the NCMLP takes a neocognitron that has been trained using SHOP and replaces the final layer C-cells with a two layer MLP (Fig. 21). The MLP portion of the network is then trained to associate the outputs of the final layer S-cells with a single output that represents the class of the input image.

A. NCMLP Implementation Issues

On top of the variables attendant to the neocognitron, the NCMLP requires the experimenter to specify learning rate (η), momentum (α), number of hidden units, initial random weight variance, etc. One consolation is that the sheer volume of research involving MLP systems provides some empirical guidelines for selecting these parameters. But regarding the number of hidden units needed for the task at hand, the only practical answer seems to be to evaluate a variety of network architectures and choose the one that offers the best generalization performance (much in the same way that SHOP settles upon good selectivity values).

B. Experiments with the NCMLP

NCMLP training involves two phases: the first uses SHOP to determine effective selectivities for the neocognitron portion of the network; the second uses validation techniques in conjunction with backpropagation to determine the structure and weights for the MLP section.

We used SHOP and a validation set of 400 unthinned CEDAR digits to find selectivities for the DL-1992 network ($R_{\text{best}} = \{1.700, 1.602, 1.000, 1.000\}$). Determining an ap-

propriate architecture for the MLP portion of the network was more involved.

To ensure inputs would not be classified on the basis of low or ambiguous outputs, we applied two thresholds, $t_{\text{val}} = 0.9$ and $t_{\text{conf}} = 0.1$, to the outputs of the NCMLP. t_{val} denotes the *threshold of validity* and t_{conf} the *threshold of confusion*. For a given test digit, if no final layer unit's output was above t_{val} or more than one unit's output was above t_{conf}, the digit was rejected. Otherwise, the digit was classed according to the unit with the highest output.

As well as thresholds to ensure rejection of illegible or ambiguous digits, the NCMLP was *trained* to reject images of ill-formed digits. Bromley and Denker [25] advocate the training of MLP type classifiers with "rubbish" subimages (i.e., ambiguous digits, multiple or partial digits, and noise) to enhance rejection performance. The set of digits used to train the MLP portion of the network contained 440 examples of each digit[11] and 440 "rubbish" images.

Ten different MLP structures were evaluated; each had 207 inputs (23 US4 planes, each with 3×3 cells) and ten outputs, and the number of hidden units varied between each network from five, ten, 15, $\cdots$, up to 50 units. Backpropagation training was applied to all networks using a learning rate of 1.0 and a momentum of 0.9. The performance of each architecture during training was monitored using a validation set of 4400 digits.[12]

Under the assumption that validation set performance correlated highly with generalization ability,[13] the most effective MLP was the one that achieved the highest classification rate on the validation set. This turned out to be a network with 45 hidden units, after 280 epochs of training. The test set[14] performance of this NCMLP is shown in row 9 of Table I.

There is an inherent difficulty in comparing the NCMLP's performance to other digit recognition systems. As Suen *et al.* point out in their survey "... recognition systems cannot be compared simply by their reported performances since most systems are still tested on data bases with very different characteristics." [22, p. 1176]. For practical reasons, we cannot evaluate the NCMLP's performance on each of the data sets mentioned by Suen *et al.*, however, their survey does cite results obtained by Cohen *et al.* on the 2711 test digits of the CEDAR database [26]. The 95.54% correct recognition rate (with 97.97% reliability) was achieved by Cohen *et al.* via a combination of four recognition algorithms, so it is unfair to compare the NCMLP with this result. Unfortunately, Cohen *et al.* only report the results of three of their individual recognizers and, to further complicate the issue, different sizes of test set were used in measuring results. We present Table II to give *an impression* of how the NCMLP fares against the systems used in [26].

[11] Taken from the `TRAIN/BINDIGIS/BR` section of the CEDAR CD-ROM.

[12] Again taken from the `TRAIN/BINDIGIS/BR` section of the CEDAR CD-ROM.

[13] An assumption justified by the correlation between validation and test set performances—$\rho > 0.98$ for the ten different MLP's.

[14] An unbalanced test set of 2711 digits was taken from the `TEST/BINDIGIS/BS` section of the CEDAR CD-ROM.

TABLE II
SUMMARY OF DIGIT RECOGNITION RESULTS OBTAINED BY COHEN *et al.* {26} USING THE CEDAR DATABASE

Method of analysis	Test set size	% Correct	% Reliability
Boundary	2418	86.6%	87.38%
Stroke	540	85.0%	90.42%
Contour	2418	79.7%	80.89%

Since submission of this manuscript, it has been brought to our attention that Fukushima *et al.* have independently developed a selectivity hunting method like SHOP [27], [28]. Using this algorithm with an expanded network, bend detection cells, modified S-cell response functions, and a mixture of supervised and unsupervised learning, Fukushima *et al.* achieve a correct recognition rate of 97.3% on 3000 digits from the ETL-1 database (published by the Electrotechnical Laboratory, Japan). Again, it is not possible to make a fair comparison of the NCMLP's performance on CEDAR digits with a system tested on ETL-1 data, but it is interesting to note that Fukushima has found a SHOP-like approach to selectivity adjustment worthwhile.

While looking for ways to raise the NCMLP's performance further still, it became clear that the neocognitron section of the network was not extracting all the features necessary for the MLP to distinguish between certain classes of digit. Additional training of the MLP would not remedy this situation; the feature extraction process would have to be altered either 1) by retaining the NCMLP paradigm and designing a more effective feature extraction network or 2) by rejecting the NCMLP model and trying to develop a system with a greater ability to learn to exploit distinguishing features of digits. The time and effort needed to redesign and retest the NCMLP renders the first option impractical. The second alternative has already been explored by Le Cun *et al.* [29], [30] who have applied gradient descent techniques and second derivative pruning methods to a hierarchical network very similar in structure to the neocognitron.

At this point we believe we have gone as far as possible in our investigation of the neocognitron and networks that are recognizably derived from it (yet distinct from existing systems). Our experiments have pointed us away from Fukushima's method of supervised training with digit fragments toward more effective, performance-driven learning schemes (i.e., gradient descent style training). But, given the success of the NCMLP and the system described by Le Cun *et al.*, it seems likely that Fukushima's concept of a hierarchy of shared-weight feature extractors will be used in the classification of images by artificial neural networks for some time to come.

VII. CONCLUSIONS

In this paper we have critically reviewed the formulation and capabilities of Fukushima's neocognitron. To the best of the authors' knowledge, this is the first time an empirical

assessment of the neocognitron with a substantial set of publicly available test data has been published.

The neocognitron's performance has been shown to be highly dependent upon the selectivity of the feature extracting S-cells and we have presented and evaluated two methods to set these parameters. The first technique, SOFT, avoids the shortcomings of Hildebrandt's OCFT algorithm by setting selectivity such that S-cells produce a guaranteed minimum response to their training patterns. Experiments with SOFT led to the proposal of SHOP, a selectivity adjustment algorithm that relies upon a validation set of real-world digits to determine effective selectivities.

Analysis of final layer S-cell outputs after training with SHOP showed that classification implemented in the final layer of the network did not fully utilize the distinguishing features extracted in preceding stages. We addressed this problem with an extension to the neocognitron which uses an MLP as the final layer classifier. We showed how this NCMLP architecture could be trained using SHOP and backpropagation, as well as a validation set of digits to determine an appropriate number of hidden units for the MLP portion of the network.

Clearly, the peak test performance of the NCMLP (84.73% correct with 96.43% reliability) was a significant improvement upon Fukushima's original network. One factor which appears to limit the NCMLP's recognition rate was the failure of the neocognitron section of the network to fully exploit the features which distinguish different classes of input. This is not necessarily a failure of the neocognitron model *per se*. While most of this paper has focussed on methods to adjust the neocognitron's parameters to maximize performance, we have not addressed the issue of how to select a training set of digit fragments that will give optimal recognition. This issue is one of the reasons why we are unable to give an exact statement of the neocognitron's performance on real-world digits. (Other reasons include the infinite variety of feasible network architectures and the multitude of data sets that could be used to test the system.)

Results presented in Section V-C show, without doubt, that skillful choice of training set enhances recognition. But this requires a degree of human intervention that is somewhat at variance with the original principles of self-organization described in Fukushima's seminal papers, and indeed, much of the machine learning ethos. Whether this is of *practical* significance to those conducting research into the supervised, unsupervised, and selective attention versions of the neocognitron will depend on the objectives of the researcher.

ACKNOWLEDGMENT

The authors gratefully acknowledge the comments and suggestions of this paper's anonymous reviewers.

REFERENCES

[1] K. Fukushima, "Neural-network model for a mechanism of pattern recognition unaffected by shift in position—neocognitron," *Trans. IECE Japan*, vol. 62-A, no. 10, pp. 658–665, 1979.

[2] K. Fukushima, S. Miyake, and T. Ito, "Neocognitron: A neural-network model for a mechanism of visual pattern recognition," *IEEE Trans. Syst., Man, Cybern,*, vol. SMC-13, 1983.

[3] K. Fukushima, "Neocognitron: A heirarchical neural-network capable of visual pattern recognition," *Neural Networks*, vol. 1, pp. 119–130, 1988.

[4] K. Fukushima and N. Wake, "Handwritten alphanumeric character recognition by the neocognitron," *IEEE Trans. Neural Networks*, vol. 2, pp. 355–365, May 1991.

[5] ———, "An improved learning algorithm for the neocognitron," in *Artificial Neural Networks*, vol. 2, I. Aleksander and J. Taylor, Eds. Amsterdam, The Netherlands: Elsevier, 1992, pp. 497–504.

[6] ———, "Improved neocognitron with bend detecting cells," in *IEEE/INNS International Joint Conference on Neural Networks*, Baltimore, 1992, vol. 4, pp. 190–195, IEEE Press.

[7] K. Fukushima, "Improvement of the neocognitron and the selective attention model," in *Proc. World Congr. Neural Networks*, Portland, OR, vol. 3, 1993, pp. 634–647.

[8] D. H. Hubel and T. N. Wiesel, "Receptive fields, binocular interaction and functional architecture in the cat's visual cortex," *J. Physiology*, vol. 160, pp. 105–154, 1962.

[9] R. Hecht-Nielsen, *Neurocomputing*. Reading, MA: Addison-Wesley, 1990.

[10] A. I. Wasserman, *Neural Computing: Theory and Practice*. New York: Van Nostrand Reinhold, 1989.

[11] E. Barnard and D. Casasent, "Shift invariance and the neocognitron," *Neural Networks*, vol. 3, pp. 403–410, 1990.

[12] K. Fukushima and S. Miyake, "Neocognitron: A new algorithm for pattern recognition tolerant of deformations and shifts in position," *Pattern Recognition*, vol. 16, no. 6, pp. 455–469, 1982.

[13] K. Johnson, C. Daniell, and J. Burman, "Feature extraction in the neocognitron," in *Proc. Int. Joint Conf. Neural Networks*, vol. 2, 1988, pp. 117–126.

[14] K. Fukushima, "Analysis of the process of visual pattern recognition by the neocognitron," *Neural Networks*, vol. 2, pp. 413–420, 1989.

[15] T. H. Hildebrandt, "Optimal training of thresholded linear correlation classifiers," *IEEE Trans. Neural Networks*, vol. 2, pp. 577–588, Nov. 1991.

[16] D. R. Lovell, A. C. Tsoi, and T. Downs, "Comments on 'Optimal training of thresholded linear correlation classifiers,'" *IEEE Trans. Neural Networks*, vol. 4, pp. 367–368, 1993.

[17] D. R. Lovell, *The Neocognitron as a System for Handwritten Character Recognition: Limitations and Improvements*, Ph.D. dissertation, Univ. Queensland, Brisbane, Australia, July 1994, available FTP: archive.cis.ohio-state.edu directory: pub/neuroprose/Thesis

[18] D. Simon, private communication, June 1992.

[19] R. Fenrich and J. J. Hull, "Concerns in creation of image databases," in *Proc. Int. Wkshp. Frontiers in Handwriting Recognition*, 1993, pp. 112–121.

[20] N. J. Naccache and R. Shinghal, "SPTA: A proposed algorithm for thinning binary patterns," *IEEE Trans. Syst., Man, Cybern.*, vol. 14, no. 3, pp. 409–418, May/June 1984.

[21] S. Mori, C. Y. Suen, and K. Yamamoto, "Historical review of OCR research and development," *Proc. IEEE*, vol. 80, no. 7, pp. 1029–1058, 1992.

[22] C. Y. Suen, C. Nadal, R. Legault, T. A. Mai, and L. Lam, "Computer recognition of unconstrained handwritten numerals," *Proc. IEEE*, vol. 80, no. 7, pp. 1162–1180, 1992.

[23] A. M. Chiang and M. L. Chuang, "A CCD programmable image processor and its neural network applications," *IEEE J. Solid-State Circuits*, vol. 26, pp. 1894–1901, 1991.

[24] S. Geman, E. Bienenstock, and R. Doursat, "Neural networks and the bias/variance dilemma," *Neural Computa.*, vol. 4, pp. 1–58, 1992.

[25] J. Bromley and J. S. Denker, "Improving rejection performance of handwritten digits by training with 'rubbish,'" *Neural Computa.*, vol. 5, pp. 367–370, 1993.

[26] E. Cohen, J. J. Hull, and S. N. Srihari, "Understanding handwritten text in a structured environment: determining ZIP codes from addresses," *Int. J. Pattern Recognition and Artificial Intell.*, vol. 5, nos. 1–2, pp. 221–264, 1991.

[27] K. Fukushima and M. Tanigawa, "Use of different thresholds in learning and recognition," *Neurocomputing*, vol. 11, no. 1, pp. 1–17, 1996.

[28] K. Fukushima, K. Nagahara, H. Shouno, and M. Okada, "Training neocognitron to recognize handwritten digits in the real world," in *Proc. World Congr. Neural Networks*, San Diego, CA, 1996, pp. 21–24.

[29] Y. Le Cun, B. Boser, J. S. Denker, D. Henderson, R. E. Howard, W. Hubbard, and L. D. Jackel, "Backpropagation applied to handwritten zip code recognition," *Neural Computa.*, vol. 1, pp. 541–551, 1989.

[30] Y. Le Cun, B. Boser, J. S. Denker, D. Henderson, R. E. Howard, W. Hubbard, and L. D. Jackel, "Handwritten digit recognition with a back-propagation network," in *Advances in Neural Information Processing Systems*, D. S. Touretzky, Ed. San Mateo, CA: Morgan Kaufmann, vol. 2, 1990, pp. 396–404.

David R. Lovell (S'89–M'89) received the Bachelor of Engineering degree in computer systems (Hons. I) and Ph.D. degrees from the University of Queensland, Australia, in 1989 and 1994, respectively.

From 1993 to 1994 he was a Lecturer at the Department of Electrical and Computer Engineering at the University of Queensland. Since 1995, he has been employed as a Research Associate at the University of Cambridge, U.K., investigating neural network and other statistical methods for prediction of risk in obstetrics. His research interests include handwritten character recognition, feature selection methods, and the application of artificial neural networks to medical problems.

Thomas Downs (M'74) received the B.Tech. and Ph.D. degrees from the University of Bradford, U.K., in 1968 and 1972, respectively.

From 1968 to 1973 he was employed by the Marconi Company in Chelmsford, U.K., in the Theoretical Sciences Laboratory, where he worked on the computer-aided design of electrical circuits and systems. In 1973, he joined the Department of Electrical Engineering at the University of Queensland, Australia, where he is now Professor. His main research interests are in the theory and application of artificial neural networks, mathematical statistics, and applied probability modeling. He has published some 120 technical papers and is coauthor of the book *Logic Design with Pascal* (New York: Van Nostrand Reinhold, 1988).

Ah Chung Tsoi (S'70–M'72–SM'90) was born in Hong Kong. He received the Higher Diploma in electronic engineering from Hong Kong Technical College in 1969 and the M.Sc. degree in electronic control engineering and the Ph.D. degree in control engineering from the University of Salford in 1970 and 1972, respectively.

From 1972 to 1974 he worked as a Senior Research Fellow at the Inter-University Institute of Engineering Control, University College of North Wales, Bangor, Wales. From 1974 to 1977, he worked as a Lecturer at the Paisley College of Technology, Renfrewshire, Scotland. From 1977 to 1984, he worked as a Senior Lecturer at the University of Auckland, New Zealand. From 1985 to 1990, he worked as a Senior Lecturer at the University College, University of New South Wales. From 1990–1996, he was Associate Professor, and then a Professor in Electrical Engineering at the University of Queensland. Since July 1996 he has been Dean, Faculty of Informatics, University of Wollongong, Australia. His research interests include aspects of neural networks and their application to practical problems, adaptive signal processing, and adaptive control.